

IN-VITRO-SIMULATED OCCLUSAL TOOTH WEAR MONITORING BY
POLARIZATION-SENSITIVE OPTICAL
COHERENCE TOMOGRAPHY

by

Ghadeer Alwadai

Submitted to the Graduate Faculty of the School of Dentistry in partial fulfillment of the requirements for the degree of Master of Science in Dentistry, Indiana University School of Dentistry, 2019.

Thesis accepted by the faculty of the Cariology and Operative Department,
Indiana University School of Dentistry, in partial fulfillment of the requirements for the
degree of Master of Science in Dentistry.

Kim Diefenderfer

Frank Lippert

Anderson Hara
Chair of the Research Committee

Norman Cook
Program Director

Date

ACKNOWLEDGMENTS

I would like to express my special thanks and gratitude to my mentor, Dr. Anderson Hara, for his encouragement and guidance throughout this project as well as to those on my research committee, Drs. Kim Diefenderfer and Frank Lippert, for their help and support. I am also grateful for the program director, Dr. Norman Blaine Cook, who gave me the golden opportunity to be part of the Cariology and Operative dentistry family.

I will always be thankful to my parents, family, and friends for their continuous support and invaluable assistance.

I would like to express my appreciation to my sponsors, Saudi Arabian Cultural Mission (SACM) and King Khalid University, which granted me this opportunity to improve my career and provided all possible facilities.

TABLE OF CONTENTS

Introduction.....	1
Review of Literature.....	5
Methods and Materials.....	14
Results.....	27
Tables and Figures.....	29
Discussion.....	38
Conclusion.....	43
References.....	45
Abstract.....	51
Curriculum Vitae	

LIST OF ILLUSTRATIONS

TABLE I	Eccles index for erosive tooth wear.....	7
TABLE II	Tooth wear index (TWI) by Smith and Knight.....	7
TABLE III	The erosive scoring system by Lussi.....	8
TABLE IV	Basic Erosive Wear Examination (BEWE) index.....	8
TABLE V	Enamel thickness measurements of different grindings by μ -CT and PS-OCT.....	30
TABLE VI	Interclass correlation of μ -CT and PS-OCT.....	30
TABLE VII	The difference between enamel thickness of different grindings by μ -CT.....	31
TABLE VIII	The difference between enamel thickness of different grindings by PS-OCT.....	32
TABLE IX	Enamel thickness measurements of different BEWE scores by μ -CT and PS-OCT.....	33
TABLE X	Interclass correlation of μ -CT and PS-OCT.....	33
TABLE XI	The difference between enamel thickness of different BEWE scores by μ -CT.....	34
TABLE XII	The difference between enamel thickness of different BEWE scores by PS-OCT.....	35
FIGURE 1	Sectioned premolar at CEJ fixed on acrylic block with cyanoacrylate adhesive and sticky wax.....	16
FIGURE 2	Micrometer used for measurement during grinding.....	17
FIGURE 3	Struers machine used for grinding by diamond abrasive discs.....	18
FIGURE 4	PS-OCT probe fixed in positioning arm with a sample placed on adjustable table.....	19
FIGURE 5	PVS guide for easier positioning of the sample after grinding.....	20
FIGURE 6	Graph shows the position of the measurement.....	21

FIGURE 7	Example of baseline measurement of PS-OCT coronal slice.....	21
FIGURE 8	A sample covered with parafilm sheet and mounted on μ -CT rotary stage.....	22
FIGURE 9	A screen ruler on DataViewer axial section locating the cusp tip position from the buccal surface.....	23
FIGURE 10	Example of baseline measurement of μ -CT coronal image using ImageJ 1.48 software.....	23
FIGURE 11	Human lower first premolars show the different BEWE scores.....	24
FIGURE 12	Example of measurement of BEWE 1 sample on PS-OCT sagittal slice.....	25
FIGURE 13	Example of measurement of BEWE 1 sample on μ -CT sagittal image.....	26
FIGURE 14	ICC and Bland Altman Plots of μ -CT and PS-OCT (phase 1).....	36
FIGURE 15	ICC and Bland Altman Plots of μ -CT and PS-OCT (phase 2).....	37

INTRODUCTION

Erosive tooth wear (ETW) is the loss of tooth substance due to chemo-mechanical action unrelated to bacteria. ETW occurs from exposure to acids of extrinsic origins (e.g. acidic industrial vapor or diet), intrinsic origins (e.g. gastric acid), or both. This process leads to demineralization of the tooth surface, increasing its roughness. Eroded surfaces are also softer and consequently less resistant to physical forces. Therefore, the combination of erosion and abrasion leads to increased damage to the tooth structure compared to each of these phenomena alone.^{1,2} Clinically, the continuing dental exposure to acids can eventually cause morphological changes to the tooth, where the excessive enamel loss can cause its convex areas to become flat or concave. In advanced stages of ETW, dentin may become exposed, resulting in dentin hypersensitivity, acute pain, and/or pulp necrosis with apical lesion.³

ETW is a growing problem worldwide. In the U.S., the National Health and Nutrition Examination Survey (NHANES, 2003-2004) reported an estimated prevalence of 45.9 percent among children⁴ and 80 percent among adults.⁵ ETW is generally reported as a common condition in developed societies and therefore it is necessary to assess and monitor it clinically.

Many indices based on visual examination are available for the clinical assessment of ETW. The earliest index was established by Eccles in 1978,⁶ Smith and Knight in 1984 slightly modified the Eccles index and developed the tooth wear index (TWI), in which all surfaces of present teeth were scored for wear.⁷ Most of the other available indices are modifications of these indices.⁸ Another index, known as Basic

Erosive Wear Examination (BEWE), was proposed more recently by Bartlett et al. (2008).⁹ It has been validated^{10,11} and used in multiple epidemiological studies.^{12,13}

Although useful, these indices are subjective and heavily based on the clinical experience of the examiner.¹⁴ These indices require experience to allow reliable results. Dental examiners with different clinical backgrounds may have inconsistent results.⁸ Ideally, quantitative methods should be clinically available to provide objective and measurable outcomes with high degree of sensitivity and specificity.

Some quantitative techniques have been proposed and used for clinically assessing erosive tooth wear, including quantitative light-induced fluorescence (QLF), which scans the surface quickly, but has low-resolution; ultrasonic measurement, which is also nondestructive and requires no special preparation before examination, but also provides low-resolution images; and optical coherence tomography (OCT), which presents higher resolution tridimensional images, is nondestructive and noninvasive, and requires no special preparation before examination.¹⁵

It was reported that OCT is able to quantify the loss of enamel thickness in GERD patients.¹⁶ Chew et al. reported that OCT is able to detect early erosive lesions *in vitro* on the buccal surfaces of human incisors after 10 minutes of erosive challenge and to monitor its progression at the surface level.¹⁷ Also, polarization-sensitive OCT (PS-OCT) is an effective method for measuring enamel thickness on human enamel samples.¹⁸ In this study, we propose to explore the use of polarization-sensitive optical coherence tomography (PS-OCT) as a tool for the objective measurement of ETW based on enamel thickness determination, with focus on the occlusal surfaces. These surfaces seem to be

highly susceptible to erosive-abrasive challenges, making them suitable clinical indicators of ETW progression.

REVIEW OF LITERATURE

Clinical Index for Erosive Tooth Wear

Clinical assessment of ETW is still considered difficult because it progresses slowly and the available techniques generally have low sensitivity. In addition, lack of a reference point to which loss of tooth surface can be measured makes it more difficult.

Many indices based on visual examination are available for the clinical assessment of ETW. The earliest index was established by Eccles (1978), in which dental erosion lesions were classified into early, small, and advanced on the affected tooth surface⁶ (Table I). Smith and Knight (1984) slightly modified the Eccles index and developed the tooth wear index (TWI), in which all surfaces of present teeth were scored for wear⁷ (Table II). Linkosalo and Markkanen (1985) developed a scoring system to evaluate the severity of erosive lesions¹⁹ that was modified by Lussi (1996) (Table III).²⁰ Another index, known as Basic Erosive Wear Examination (BEWE), was proposed more recently by Bartlett et al. (2008), which scores all surfaces but considers only the most severely affected surface in each sextant in an attempt to determine the overall ETW level of the patient (Table IV).⁹

These indices of erosive tooth wear are shown in Table I through Table IV on the following pages.

TABLE I

Eccles index for erosive tooth wear (1978)

Class I	Smooth, glazed surface, lack of developmental ridges, mainly found on facial surfaces of upper anteriors.
Class II	Facial dentin involvement in less than one third of surface.
Class III a	Facial dentin involvement more than one third of the surface, particularly affecting anteriors.
Class III b	Lingual or palatal dentin involvement in more than one third of the surface.
Class III c	Incisal and occlusal dentin involvement.
Class III d	The severely worn teeth, extensive dentin of labial and lingual surfaces, proximal surfaces may be affected, teeth may be shortened

TABLE II

Tooth wear index (TWI) by Smith and Knight (1984)

Score	Surface	Criteria
0	B/L/O/I C	Sound. Sound.
1	B/L/O/I C	Loss of enamel surface characteristics. Minimal loss of contour.
2	B/L/O I C	Dentin exposure for less than one third of surface. Loss of enamel just exposing dentin. Defect less than 1 mm deep.
3	B/L/O I C	Dentin exposure for more than one third of surface. Loss of enamel and substantial loss of dentin. Defect less than 1 mm to 2 mm deep.
4	B/L/O I C	Complete enamel loss – pulp exposure – secondary dentin exposure. Pulp exposure or exposure of secondary dentin. Defect more than 2 mm deep – pulp exposure – secondary dentin exposure.

* B: buccal, L: lingual, O: occlusal, I: incisal, C: cervical.

TABLE III

The erosive scoring system by Lussi (1996)

Score	Facial Surface Criteria
0	No erosion, smooth, glazed surface, possible lack of developmental ridges.
1	Loss of surface enamel; intact cervical, and no dentin exposure.
2	Dentin exposure for less than half of the tooth surface.
3	Dentin exposure for more than half of the tooth surface.
Score	Occlusal and Lingual Surfaces Criteria
0	No erosion, smooth, glazed surface, possible lack of developmental ridges.
1	Slight erosion, loss of enamel surface, rounded cusps, edges of restorations rising above the level of the adjacent tooth surface, no dentin exposure.
2	Severe erosions, more pronounced signs than in grade 1, dentin exposure.

TABLE IV

BEWE index (Bartlett et.al. 2008)

Score	Criteria
0	No erosive tooth wear.
1	Initial loss of surface texture.
2	Distinct defect, hard tissue loss <50% of the surface area (dentin is often involved).
3	Hard tissue loss \geq 50% of the surface area (dentin is often involved).

These indices are highly subjective and depend heavily on clinical experience in order to obtain reliable results. Dental examiners with different backgrounds usually provide different results. Therefore, those indices are not the ideal choice for the measurement of ETW.

Objective Methods for Tooth Wear Measurement

There are objective techniques that have been proposed and are used for quantifying ETW, including quantitative light-induced fluorescence (QLF). QLF depends on fluorescence of enamel, a property of which is that loss of minerals will decrease the amount of fluorescence. The demineralized areas will appear darker, allowing early detection of erosive lesions and quantitative measurement of erosion.²¹ It has been shown that QLF is able to detect and monitor erosive lesions *in vitro* by measuring the loss of fluorescence.²² QLF is nondestructive and quick, but the downside is that it provides low-resolution images.¹⁵

Ultrasonic measurement is also nondestructive and requires no special preparation before examination, but it too provides low-resolution images.¹⁵ It depends on an ultrasonic pulse that is transmitted through enamel to the dentino-enamel junction. The time for transmission of the pulse through the enamel layer is calculated by light stereomicroscope, which is used for enamel thickness estimation.²³ It has been demonstrated that enamel thickness can be measured by ultrasound to monitor erosive lesions *in vitro*.²⁴ However, its use for ETW measurement is limited due to poor reliability in measuring less than 300- μ m change in enamel thickness, something caused in part by poor probe positioning and difficulties in repeating measurements.²⁵

Mair et.al.²⁶ proposed that the best method for evaluation of tooth wear is comparing consecutive 3D images of the tooth, which involves 3D scanning the teeth, superimposing a new image onto the previous scan, and then measuring the difference in volume. Only very few studies have used this method due to the high cost of 3D scanning machines. Park et al. used this method to evaluate tooth wear that occurs during

orthodontic treatment and found it is a useful method for quantitative measurement of tooth wear in orthodontic patients.²⁶

Micro Computed Tomography (μ -CT), also called microtomography, x-ray microscopy, or CT scanning,²⁷ is nondestructive, high-resolution 3D imaging x-ray technology. It is similar to medical CT, but with higher resolution and a smaller scale. Medical CT was introduced in the 1970s with a maximum of 70- μ m resolution, while μ -CT was later introduced in the 1980s and has resolution ranging from 5 μ m to 150 μ m.²⁸ The process of μ -CT involves the presence of an x-ray source, a detector, and a sample. The x-ray source and the detector are fixed while the sample rotates. First, a cone beam x-ray is emitted from the source to the rotating sample, creating a shadow image of the sample on the detector. The detector then collects the 2D images of the sample, and finally, reconstruction software is used to develop the 3D images of the sample.²⁷ Despite the advantages of μ -CT, it has limitations in that it is almost limited to micro sizes; it involves no chemical analysis, and it requires significant experience to obtain useful data.²⁷

However, μ -CT has been used in different aspects of dental studies, such as for measurement of enamel thickness.^{29,30} It was concluded that μ -CT is an accurate and reliable method for measuring enamel thickness, taking into consideration the difficulty of distinguishing between dental tissues of severely mineralized teeth and differentiating the very thin enamel (less than 100 μ m).³⁰ When μ -CT was compared with direct measurement, photography, and 3D scanning, it was found to be a more reliable method for measuring distances on both internal and external tooth structures.³¹ It also had been used to analyze the pulp cavity, allowing researchers to observe the shape of the pulp

cavity, the volume ratio of the pulp horns, the volume of the pulp chamber, and the diameter of the orifices.³² Furthermore, this method was used to observe the characteristics of C-shaped canals.³³ Micro computed tomography was also used to assess periapical lesions in animals,³⁴ and it was concluded that μ -CT is a meticulous method for morphometric evaluation and volumetric scanning.³⁵

OCT (Optical Coherence Tomography) is a nondestructive, noninvasive (no ionizing radiation), and relatively high-resolution imaging technology that uses near-infrared light to produce 3D scans. It was first introduced by the IT department of Massachusetts University in 1991³⁶ and first used *in vivo* for retinal measurements in Vienna in 1993.³⁷ In 1996 (Zeiss) Humphrey produced the first commercial OCT. The first use of OCT on teeth was in 1998 in a collaboration between the medical research laboratory of Livermore and Connecticut University.³⁸ Two years later, the same group presented the first intraoral scans for both hard and soft tissues.³⁹

The technique of OCT involves detecting and measuring the intensity of the backscattered light of an object. OCT has a cross-sectional resolution less than 10 μ m. There are two basic types of OCT: a time domain, which produces low quality 2D images of the object (no 3D images); and the more recent Fourier domain, which produces 3D images more than 100 times faster.⁴⁰ Based on the method of detection of optical frequency signals, OCT can be classified into either spectral optical coherence tomography (SOCT) or swept source optical coherence tomography (SS-OCT) [or can be named optical Fourier domain imaging (OFDI)]. SOCT produces broadband light and uses a spectrometer to detect optical frequency signals, while SS-OCT produces narrow light with better object penetration and uses a photodetector to detect optical frequency

signals.⁴⁰ Polarization-sensitive optical coherence tomography (PS-OCT) is a development of SS-OCT. It has the advantage of improved contrast of the images based on the polarization state of the object's backscattered light. One of the limitations, however, of OCT is that it requires experience to visualize and measure images. Additionally, the resolution of OCT images still can be considered a limitation.

OCT has been used for various purposes in dental research. Some of these include assessment and progression monitoring of enamel early caries lesions,^{41,42,43} root caries,⁴⁴ and caries under restorations.⁴³ Furthermore, OCT was used in endodontics, showing high sensitivity and specificity for the diagnosis of vertical root fractures and becoming a non-ionizing alternative method for vertical root fracture diagnosis.^{45,46} OCT was also used to evaluate the periodontal ligaments during application of different orthodontic forces. The findings of these studies supported the use of OCT for monitoring the PDLs during orthodontic treatments.^{47,48} Another subject of evaluation was the assessment of marginal adaptation, internal integrity, and porosity of resin restorations in which the high resolution of OCT was helpful in providing important information about the structure of resin restorations.^{49,50} Additionally, linear polymerization shrinkage of different resins was also evaluated using OCT.⁵¹ Moreover, when cracks were assessed by OCT and compared to histological sections, OCT was able to distinguish them as highlighted lines due to the reflected light, and there was a strong correlation between the OCT and the histological sections regarding the dimensions of the cracks.⁵² OCT was used to quantify remaining dentin thickness of occlusal cavities⁵³ and thickness of human buccal and lingual enamel samples,¹⁸ suggesting OCT as an effective clinical method for

such measurements. Finally, OCT was also used in periodontics, and it was able to visualize the deep pockets in porcine jaws.⁵⁴

From the current literature, OCT is a reliable method for measurement of enamel thickness on smooth surfaces¹⁸ as well as monitoring tooth wear progression.¹⁷ The literature is lacking measurement of enamel thickness and assessment of ETW using OCT on occlusal surfaces. It is important to assess the use of OCT on occlusal surfaces due to the difference in anatomical structure from the smooth surfaces. Also, occlusal surfaces are good clinical indicators for ETW progression due to the faster progression. Therefore, the purpose of this study is to explore the use of PS-OCT for measurement of enamel thickness and monitoring tooth wear progression focusing on occlusal surfaces.

MATERIALS AND METHODS

EXPERIMENTAL DESIGN

This study is presented in two phases. In the first phase, 10 sound extracted human lower first premolars were selected and exposed to tooth wear simulation gradually. PS-OCT and μ -CT were used to evaluate enamel thickness at the buccal cusp tips of the premolars. In phase 2, 40 extracted human lower first premolars with different severity levels of erosive tooth wear on occlusal surfaces (based on BEWE index) were selected. PS-OCT and μ -CT were used to evaluate the enamel thickness and the results were compared to their BEWE scores.

PHASE 1

Teeth Selection and Preparation

Ten sound extracted human lower first premolars were randomly collected from a teeth bank at the Oral Health Research Institute (OHRI), Indiana University School of Dentistry (IRB #: NS0911-07). Patient information and extraction reasons were not recorded, rendering all samples to be completely unidentified. It is assumed that most of the teeth were extracted due to orthodontic or periodontal reasons, and their collection was performed over years from several dental practice clinics across the United States. Upon receipt at OHRI, teeth were sorted, cleaned, and kept in thymol 0.1 percent, at 4° C. Teeth with carious lesions, restorations, and broken crowns due to extraction were excluded. After collection, all teeth were cleaned using periodontal scalers. Each tooth was placed in a labeled vial containing thymol 0.1 percent. They were sectioned at CEJ

and the crown portion fixed on 1x1 cm acrylic blocks by cyanoacrylate adhesive and sticky wax for tooth wear simulation.



FIGURE 1. Sectioned premolar at CEJ fixed on acrylic block with cyanoacrylate adhesive and sticky wax.

Tooth Wear Simulation

The buccal cusp tip of each tooth was abraded using diamond abrasive discs (500-, 1200-, 2400-, and 4000-grit Al_2O_3 papers (MD-Fuga, Struers Inc, Cleveland, OH, USA) to remove 0.5 mm, 1 mm, and 1.5 mm of enamel. The amount of enamel ground away was measured using an electronic micrometer and recorded individually. Measurements using PS-OCT and μ -CT were performed at the baseline and after each tooth wear simulation (enamel removal of 0.5 mm, 1 mm, and 1.5 mm).



FIGURE 2. Micrometer used for measurement during grinding.



FIGURE 3. Struers machine used for grinding by diamond abrasive discs.

PS-OCT Measurement

The premolar to be scanned was removed from the storage container, gently dried using delicate task wipers (Kimwipes, Kimberly-Clark Corp.), and positioned under the sensor of the PS-OCT probe (Santec Inner Vision IVS-300; Santec Corp, Komaki, Japan), with the occlusal surface oriented toward the sensor of the probe and the lingual surface oriented toward the probe handle with the probe fixed in a positioning arm. The sensor of the probe was covered with a plastic wrap and secured with a rubber band for the purpose of infection control. A 3D scan by Inner vision software (5 mm x 5 mm x 5.6 mm) was performed for each tooth with the buccal cusp centered in the middle of the scan window. The lateral and axial resolutions were 20 μm and 5.5 μm , respectively, at a

refractive index of 1.6. From the 3D scan, the central 2D coronal slice showing the buccal cusp tip was selected and saved for measurements. A localization guide with PVS impression material (EXAMIX, GC America Inc. ALSIP, IL, USA) was made for each tooth after the baseline scanning to be used as a reference for easier positioning of the tooth for scanning after each wear. The PVS guide captured the buccal surface of the premolar, the acrylic block, and the head of probe. The specimens were kept in 0.1-percent thymol containers at all times except during measurement procedures (including positioning and scanning), which were performed within 3 min in order to ensure their adequate hydration level.

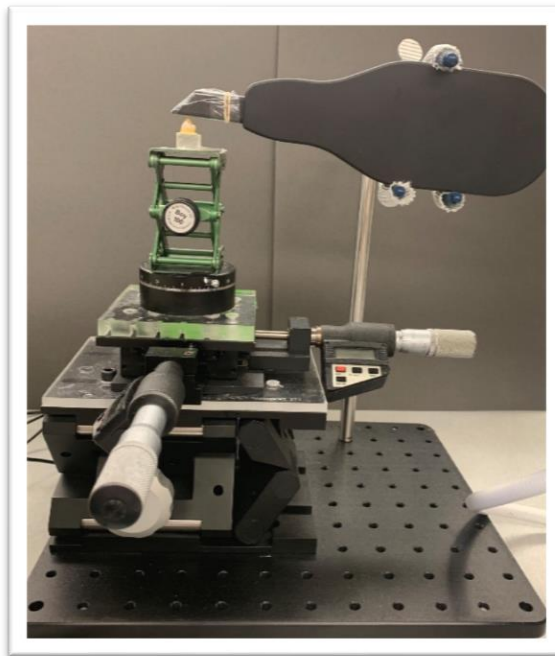


FIGURE 4. PS-OCT probe fixed in positioning arm with sample placed on adjustable table.

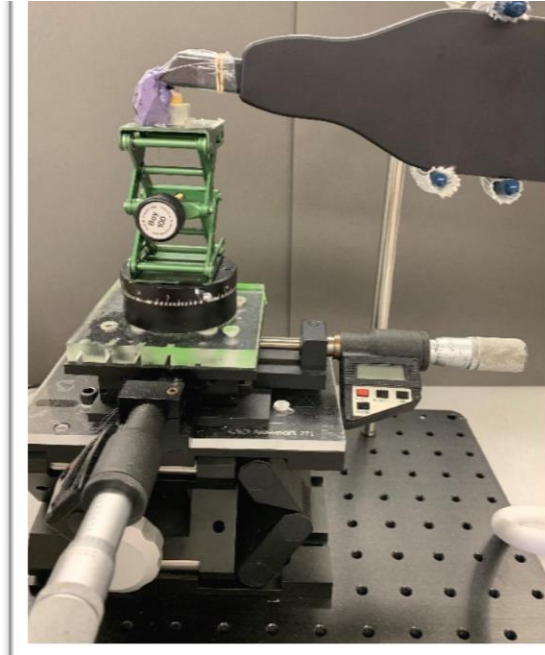


FIGURE 5. PVS guide for easier positioning of the sample after grinding.

Enamel Thickness Analysis

The acquired 2D images were randomized and the examiner was blind about the wear condition to avoid bias. Each image was labeled using the annotation tool of the Inner Version software. The buccal cusp tip was labeled using the annotation tool, which has horizontal and vertical lines intersecting at a point. The DEJ was visually determined under the cusp tip and marked with the annotation tool. The intensity measurement function on PS-OCT was used to detect the highest intensity peaks corresponding to the annotation marks that represented the enamel surface and DEJ areas. It was then used to measure the distance between them. The distance between the two peaks was recorded in mm to represent the enamel thickness measurement at the buccal cusp tip. PS-OCT scanning and measurement procedures were performed by one trained examiner at the baseline and following each erosive simulation.

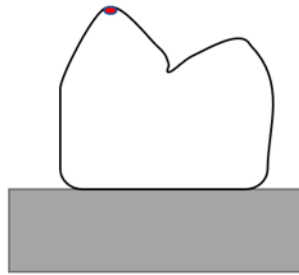


FIGURE 6. Graph shows the position of the measurement.

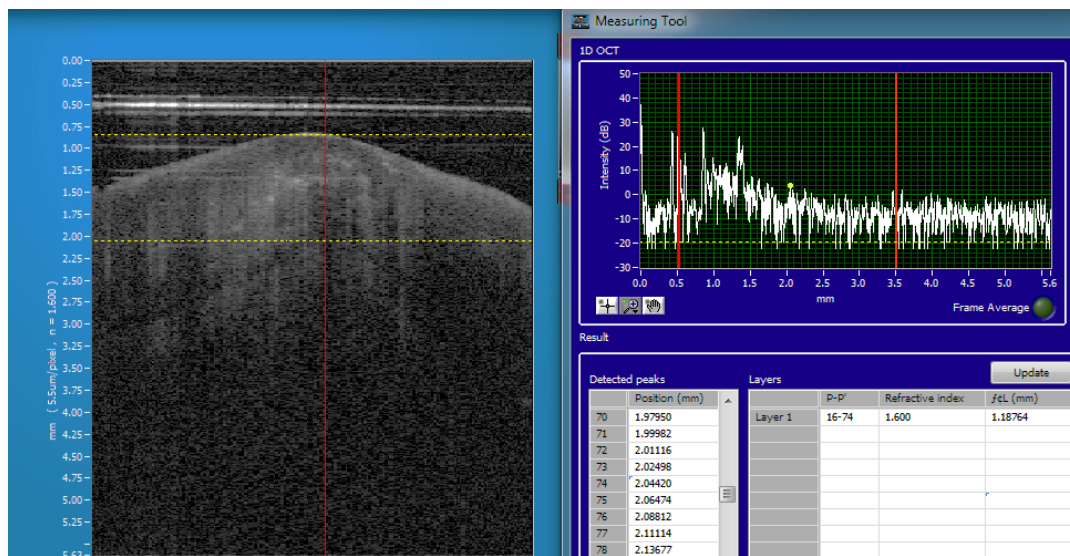


FIGURE 7. Example of baseline measurement of PS-OCT coronal slice.

μ -CT Measurement

The premolars were scanned with μ -CT (Skyscan1172; Bruker micro CT, Kontich, Belgium). Specimens were mounted on a rotary stage and covered with parafilm sheets (PARAFILM “M”, Bemis) to avoid dehydration during scanning. They were then subjected to an X-ray beam (59 kV / 167 uA) perpendicular to the long axis of the premolars. A 0.5-mm aluminum filter and medium camera with 6- μ m pixels were used. Images were saved in TIFF format and reconstructed into 3D models with 2000 \times 2000-

pixel resolution. Reconstructions were done using Skyscan NRecon software. DataViewer was used to detect the highest point on the occlusal surface (the buccal cusp tip) and to obtain the coronal image at the cusp tip. A screen ruler was used on the DataViewer axial section at the highest contour of each tooth to determine the position of the cusp tip from the buccal and proximal height of the contour. The ruler was then used as a reference for the cusp tip position in the subsequent scans of the tooth. The coronal images were randomized and the examiner was blind about the wear condition. Finally, enamel thickness (surface-DEJ distance) at the cusp tip was measured using ImageJ 1.48 software.

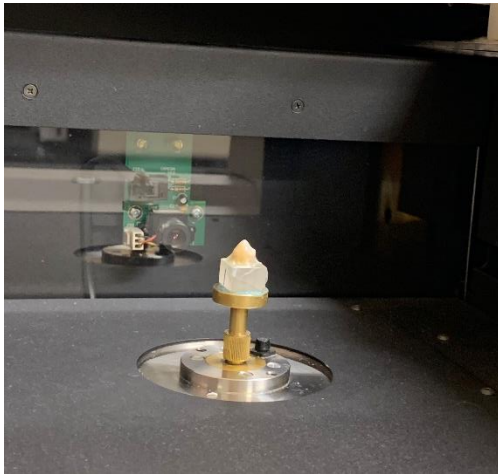


FIGURE 8. Sample covered with parafilm sheet and mounted on a Micro CT rotary stage.

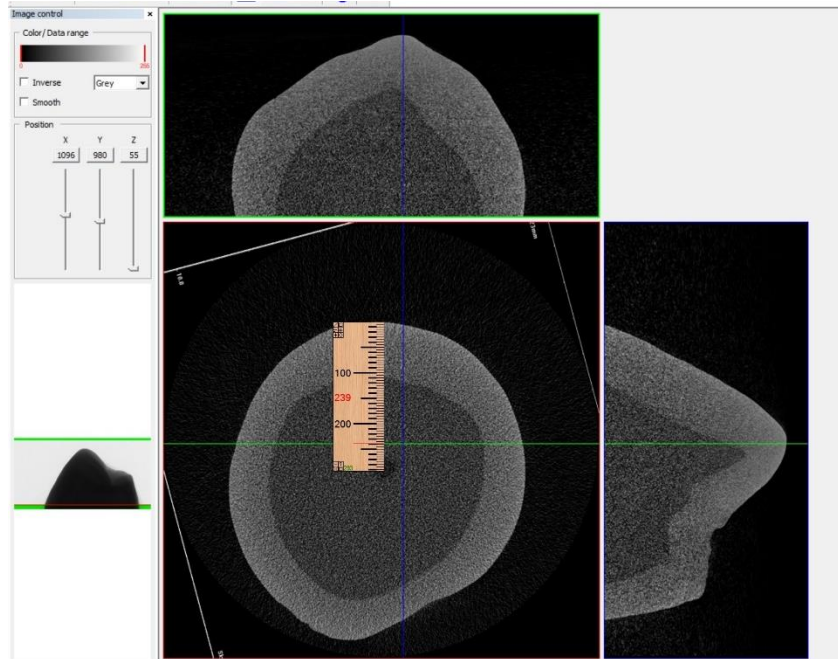


FIGURE 9. A screen ruler on a DataViewer axial section locating the cusp tip position from the buccal surface.

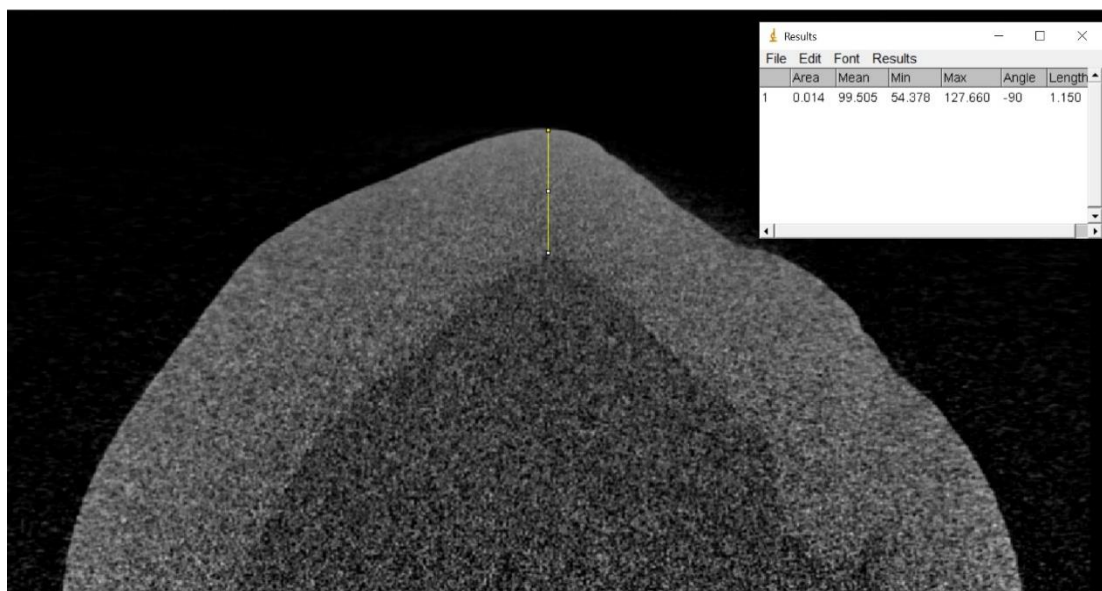


FIGURE 10. Example of baseline measurement of a μ -CT coronal image using ImageJ 1.48 software.

PHASE 2

Teeth Selection and Preparation

Forty extracted human lower first premolars were collected from a teeth bank at the Oral Health Research Institute (OHRI), Indiana University School of Dentistry. They had 10 representative samples from different BEWE scores: 0 (no surface loss), 1 (initial loss of enamel surface texture), 2 (distinct defect; hard tissue loss less than 50 percent of the surface area) and 3 (hard tissue loss more than 50 percent of the surface area) (Figure 4). The teeth were sectioned at CEJ, then the coronal part was fixed with cyanoacrylate adhesive and sticky wax on a 1x1 cm acrylic block. The enamel thickness of the occlusal surface of these premolars was then analyzed using PS-OCT and μ -CT at the buccal cusp tip.

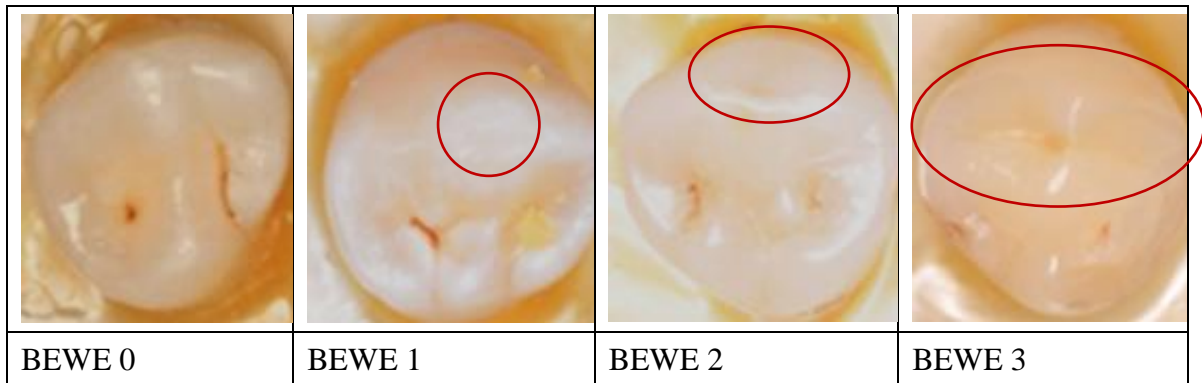


FIGURE 11. Human lower first premolars show the different BEWE scores.

Erosive Tooth Wear (ETW) Examination

The severity of ETW was scored on occlusal surfaces based on the Basic Erosive Wear Examination (BEWE) index as described by Bartlett et al. (2008). The index is displayed in Table IV.

BEWE Training

The examiner participated in a detailed three-hour presentation and discussion on BEWE severity and location scores. The training also included examination of several cases via slide presentation, representing all severity and location scores of the BEWE index. After that, the exercise was conducted on 40 extracted teeth with a senior examiner. Inter- and intra-examiner repeatability values were 0.69 and 0.86, respectively.

PS-OCT Scanning and Measurement

The teeth were scanned, and enamel thickness at the highest point of the occlusal surface on the sagittal image was measured by the same methods described in Phase 1.

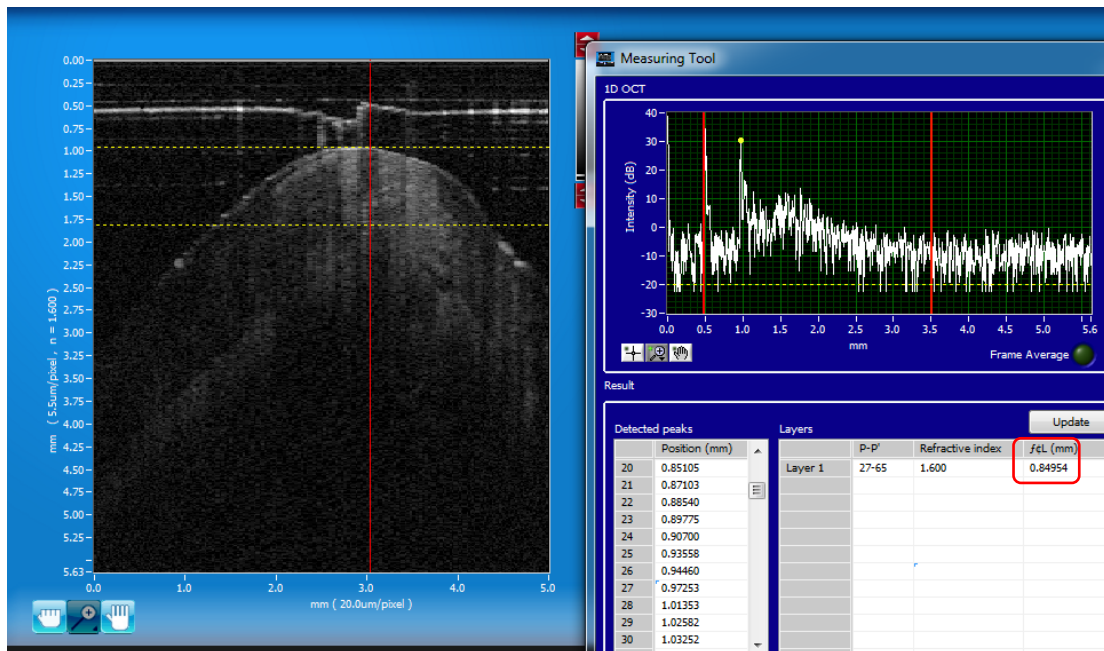


FIGURE 12. Example of measurement of BEWE 1 sample on PS-OCT sagittal slice.

μ -CT Measurement

The teeth were scanned, and enamel thickness at the highest point of the occlusal surface on the sagittal image was measured by the same methods described in Phase 1.

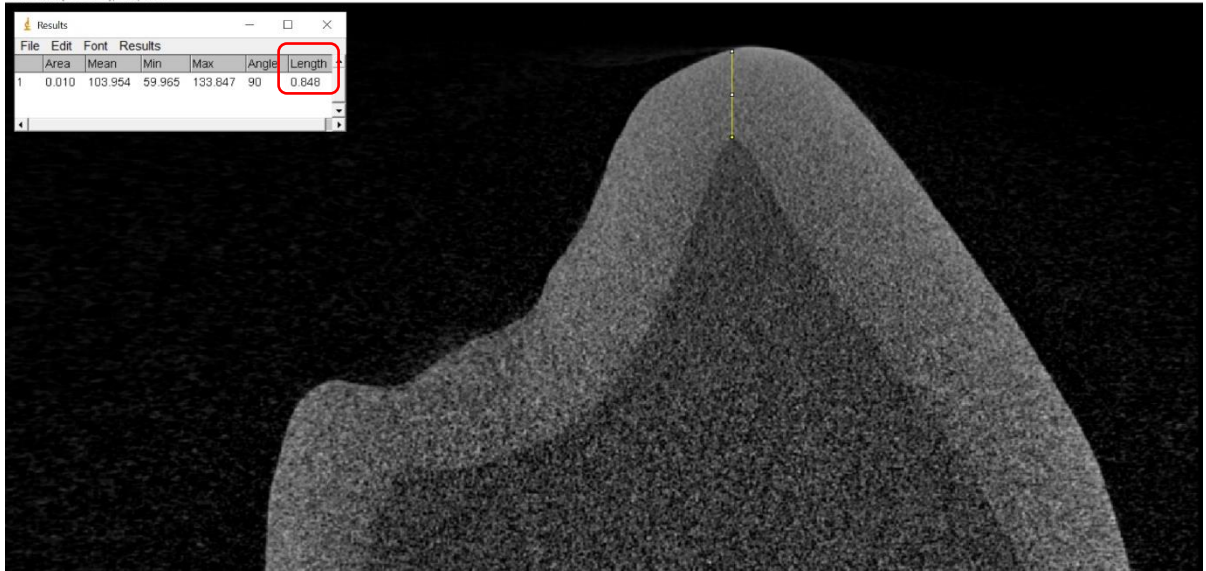


FIGURE 13. Example of measurement of BEWE 1 sample on μ -CT sagittal image.

RESULTS

PHASE 1

As can be seen in Table 6, good agreement was found between mean enamel thickness measurements by μ -CT and PS-OCT with an interclass correlation of 0.89 and no significant difference between them (p : 0.4054). No specific pattern of agreement was observed in the Bland-Altman plot (Figure 14). There were significant differences between the enamel thickness of different grindings using μ -CT (TABLE VII; all $p < 0.0001$) and PS-OCT (TABLE VIII; all $p < 0.0007$).

PHASE 2

Table X shows that there was strong agreement between mean enamel thickness measurements by μ -CT and PS-OCT with an interclass correlation of 0.97 and no significant difference between them (p : 0.2894). No specific pattern of agreement was observed in the Bland-Altman plot (Figure 15). There were significant differences between the enamel thickness of different BEWE scores using μ -CT (Table XI; $p < 0.02$) and PS-OCT (Table XII; $p = 0.009$), while there was no significant difference between the enamel thickness of BEWE 1 and BEWE 2 using μ -CT (Table XI; $p = 0.0748$) and PS-OCT (Table XII; $p = 0.4981$).

TABLES AND FIGURES

TABLE V

Phase 1 enamel thickness measurements (mm) of different grindings by μ CT and PS-OCT

Grinding (mm)	Method	N	Mean	SD	Median	Minimum	Maximum
0	μ-CT	10	1.334	0.328	1.163	1.034	2.021
	PS-OCT	10	1.328	0.257	1.198	1.077	1.859
0.5	μ-CT	10	0.811	0.340	0.633	0.517	1.492
	PS-OCT	10	0.737	0.187	0.754	0.466	1.071
1	μ-CT	10	0.325	0.336	0.123	0.074	0.966
	PS-OCT	10	0.332	0.182	0.318	0.127	0.664
1.5	μ-CT	10	0.098	0.207	0.000	0.000	0.522
	PS-OCT	10	0.033	0.103	0.000	0.000	0.326

TABLE VI

Interclass correlation of μ -CT and PS-OCT

Mean SE (μ -CT)	Mean SE (PS-OCT)	P-value	ICC
0.6422 (0.0862)	0.6075 (0.0862)	0.4054	0.89

TABLE VII

The difference between enamel thickness of different grindings by μ -CT

	Grinding (mm)	Grinding (mm)	Estimate	SE	P- value	Lower CI	Upper CI
Grinding size	0	1	1.0087	0.03864	<.0001	0.9294	1.0880
Grinding size	0	0.5	0.5230	0.03864	<.0001	0.4437	0.6023
Grinding size	0	1.5	1.2361	0.03864	<.0001	1.1568	1.3154
Grinding size	1	0.5	-0.4857	0.03864	<.0001	-0.5650	- 0.4064
Grinding size	1	1.5	0.2274	0.03864	<.0001	0.1481	0.3067
Grinding size	0.5	1.5	0.7131	0.03864	<.0001	0.6338	0.7924

TABLE VIII

The difference between enamel thickness of different grindings by PS-OCT

Effect	Grinding (mm)	Grinding (mm)	Estimate	SE	P-value	Lower CI	Upper CI
Grinding size	0	1	0.9961	0.06677	<0.0001	0.8591	1.1331
Grinding size	0	0.5	0.5917	0.06677	<0.0001	0.4547	0.7286
Grinding size	0	1.5	1.2958	0.06677	<0.0001	1.1588	1.4328
Grinding size	1	0.5	-0.4045	0.06677	<0.0001	-0.5415	0.2675
Grinding size	1	1.5	0.2997	0.06677	0.0007	0.1627	0.4366
Grinding size	0.5	1.5	0.7041	0.06677	<0.0001	0.5671	0.8411

TABLE IX

Phase 2 enamel thickness measurements (mm) of different BEWE scores by μ -CT and PS-OCT

BEWE (score)	Method	N	Mean	SD	Median	Minimum	Maximum
0	μ -CT	10	1.129	0.300	1.179	0.675	1.601
	PS-OCT	10	1.153	0.335	1.203	0.624	1.731
1	μ -CT	10	0.839	0.224	0.888	0.428	1.127
	PS-OCT	10	0.806	0.245	0.854	0.371	1.067
2	μ -CT	10	0.630	0.344	0.694	0.000	1.095
	PS-OCT	10	0.722	0.364	0.801	0.000	1.138
3	μ -CT	10	0.010	0.032	0.000	0.000	0.101
	PS-OCT	10	0.011	0.035	0.000	0.000	0.110

TABLE X

Interclass correlation of μ -CT and PS-OCT

Mean SE (μ -CT)	Mean SE (PS-OCT)	P-value	ICC
0.6518 (0.0775)	0.6730 (0.0775)	0.2894	0.97

TABLE XI

The difference between enamel thickness of different BEWE scores by μ -CT

Effect	BEWE score	BEWE score	Estimate	SE	P-value	Lower CI	Upper CI
BEWE score	0	1	0.2901	0.1139	0.0153	0.05906	0.5211
BEWE score	0	2	0.4991	0.1139	<0.0001	0.2681	0.7301
BEWE score	0	3	1.1186	0.1139	<0.0001	0.8876	1.3496
BEWE score	1	2	0.2090	0.1139	0.0748	-0.02204	0.4400
BEWE score	1	3	0.8285	0.1139	<0.0001	0.5975	1.0595
BEWE score	2	3	0.6195	0.1139	<0.0001	0.3885	0.8505

TABLE XII

The difference between enamel thickness of different BEWE scores by PS-OCT

Effect	BEWE score	BEWE score	Estimate	SE	P-value	Lower CI	Upper CI
BEWE score	0	1	0.3468	0.1237	0.0081	0.09592	0.5977
BEWE score	0	2	0.4315	0.1237	0.0013	0.1806	0.6824
BEWE score	0	3	1.1421	0.1237	<0.0001	0.8912	1.3930
BEWE score	1	2	0.08467	0.1237	0.4981	-0.1662	0.3356
BEWE score	1	3	0.7953	0.1237	<0.0001	0.5444	1.0462
BEWE score	2	3	0.7106	0.1237	<0.0001	0.4597	0.9615

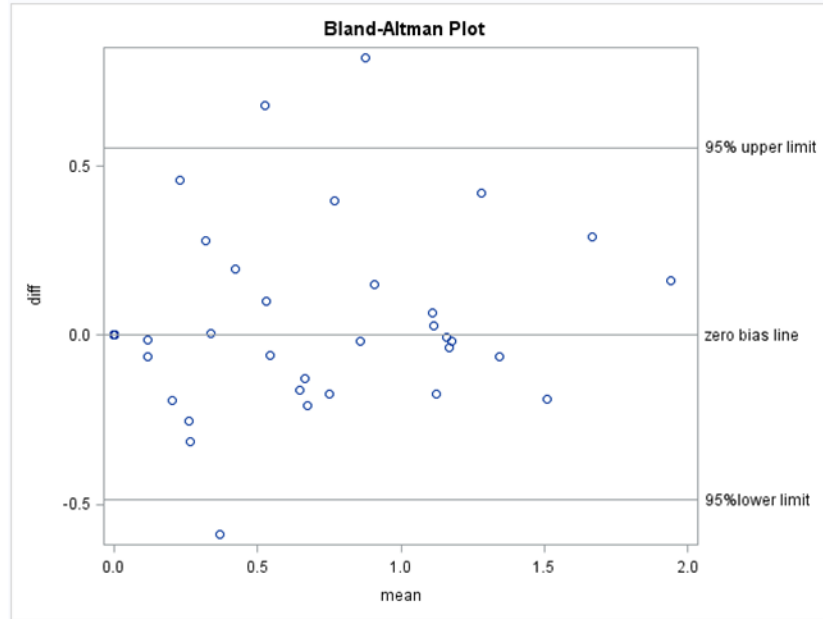


FIGURE 14. ICC and Bland Altman Plot showing no specific pattern of agreement between μ -CT and PS-OCT.

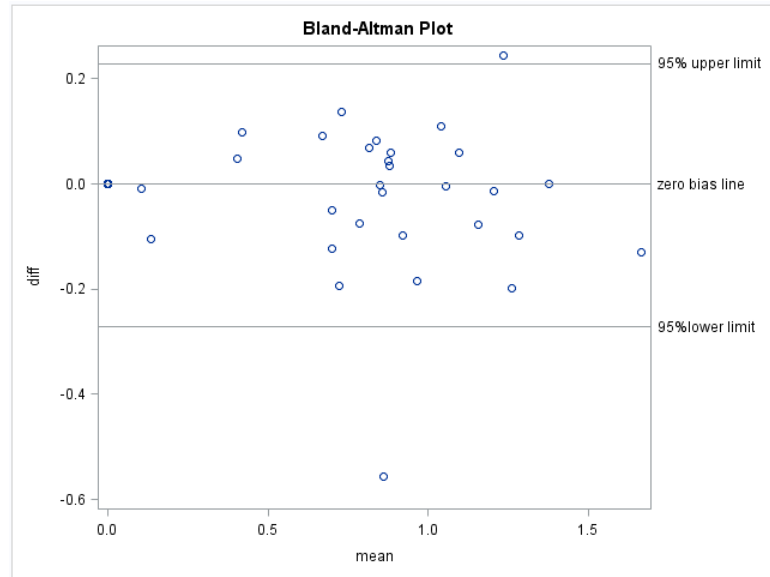


FIGURE 15. ICC and Bland Altman Plot showing no specific pattern of agreement between μ -CT and PS-OCT.

DISCUSSION

The purpose of our study was to evaluate the ability of PS-OCT to objectively measure tooth wear on the occlusal surface. Based on our results, we can accept the null hypothesis since we found good agreement between PS-OCT and μ -CT in both phases (Phase 1: 0.89 and phase 2: 0.97) with no significant difference between them. This is in agreement with previous research by Algarni et al. where excellent correlation (0.95) between PS-OCT and μ CT was found in measuring enamel thickness of smooth surfaces of extracted human teeth.¹⁸ It also agrees with the results of Majkut et al. in which strong correlation (0.96) was observed between PS-OCT and μ CT in measuring the remaining dentin of deep occlusal caries lesions in extracted human teeth.⁵³

The lower agreement in Phase 1 compared with Phase 2 can be explained by the presence of cracks that could have been created during the grinding of the cusp tips. Imai et al. showed that enamel cracks on swept source OCT were clearly distinguished as bright lines because of the increased backscattered signals.⁵⁵ We noticed bright lines in enamel on some of PS-OCT scans after the grinding. The cracks can affect light penetration through the enamel, impacting the PS-OCT measurements. Furthermore, the excellent agreement was with Phase 2, in which the wear lesions were natural.

There was a significant difference between the means of enamel thickness of different grindings in phase 1 by μ -CT (Table VII) and PS-OCT (Table VIII), which suggests that both μ -CT and PS-OCT were able to distinguish 0.5-mm changes in enamel thickness. However, in Phase 2 there was no significant difference between the means of enamel thickness of BEWE 1 and BEWE 2 by μ -CT (Table XI) and PS-OCT (Table XII).

This finding suggests that the measured enamel thicknesses of BEWE 1 and BEWE 2 were not necessarily different. That can be explained by the fact that BEWE score is based on the loss of the surface area, while our measurement was for enamel thickness at the highest point of the occlusal surface.

In the first phase, our reference point was the cusp tip since all 10 teeth were sound at the beginning of the study; a PVS guide was used to reposition each tooth after grinding (Figure 5). A coronal section at the cusp tip was used to measure the enamel thickness (Figure 7, Figure 10) and the PVS guide was utilized to standardize the section of each tooth. In the second phase, there was no reference point since we started with natural wear lesions on the cusps of 30 selected teeth (10 of BEWE 1, 10 of BEWE 2, and 10 of BEWE 3) (Figure 11), so we opted to use the highest point on the occlusal surface of these teeth as a reference point, unless there was dentin exposure. In that case, we considered the enamel thickness as zero. In this phase we used the sagittal section for measuring enamel thickness at the highest point on the occlusal surface (Figure 12, Figure 13). This was to avoid the risk of having the coronal section very facial, which would not allow us to visualize the DEJ, in presence of the highest point of the occlusal surface too far facially.

We considered μ -CT as the gold standard in our study for measurement of enamel thickness based on its well-established accuracy for linear measurements. Olejniczak and Grine found that the difference between enamel thickness measurements by μ -CT and physical sections was 3.0 percent to 5.0 percent; thus, they considered μ -CT as accurate method for enamel thickness measurements.⁵⁶ Kim et al. compared the μ -CT measurements of teeth to direct physical measurements and concluded that μ -CT is a

reliable method for linear measurements and can be used for measuring distances and observing the internal and external tooth structures.⁵⁷

Accurate measurement by OCT depends on selecting the right refractive index in order to accurately convert the optical path length to the actual thickness. In our study we measured enamel and used a refractive index of 1.6 based on Meng et al., who found that the refractive index of enamel by OCT was 1.631 ± 0.007 .⁵⁸

According to Chan et al., the prolonged dehydration of teeth leads to lack of visibility of the DEJ on OCT scans.⁵⁹ Therefore, all samples in our study were kept moist in their vials at all times except during scanning, which was limited to three minutes to avoid dehydration. Chan et al. also noticed that roughened enamel surfaces affect OCT optical penetration.⁵⁹ Therefore, after each grinding procedure with the 500-grit diamond abrasive disc, further polishing was done using 1200-, 2400-, and 4000-grit Al₂O₃ papers.

Other quantitative techniques, including ultrasound, have been used to measure enamel thickness on the occlusal surface. Bozkurt et al. measured enamel thickness of abraded cusp tips of premolars with ultrasound and compared it to histological analysis by polarized light microscopy, showing a strong correlation between the two methods (0.966).⁶⁰ PS-OCT may still be preferable for such measurements over ultrasound, which generates low-resolution images and has poor repeatability. Lee et al. used QLF to evaluate the occlusal tooth wear by measuring the difference in fluorescence intensity between sound and worn areas. They found significant differences in fluorescence intensity between sound, enamel remained and dentine exposed worn teeth, with a significant correlation between the fluorescence intensity and the wear severity.⁶¹ PS-

OCT might be superior to QLF because of its ability to directly measure the remaining enamel thickness.

This study has two primary limitations that should be taken into consideration. The first is a lack of erosive challenge. For the purpose of simplification, our study focused only on mechanical wear without acid involvement. Chan et al. found that after acid challenge, the surface roughens, leading to reduction of the optical penetration.⁵⁹ However, unpublished data from our group has shown that enamel demineralization and different surface texture did not interfere with OCT measurements. The second limitation is the lack of reference point in Phase 2 due to the natural wear of the cusp tip. As a result, we utilized the highest point on the occlusal surface as our reference point, which does not represent the most affected area.

Despite the limitations of our study, we found that PS-OCT is a reliable method to measure enamel thickness and monitor tooth wear progression on occlusal surfaces. PS-OCT is clinically applicable; the cost ranges from \$35,000 to \$100,000, and it provides a 3D scan within a few seconds. Therefore, and based on our results, we suggest the potential clinical application of PS-OCT for measuring enamel thickness and monitoring tooth wear progression on occlusal surfaces using positioning guide. Future studies considering the use of PS-OCT to evaluate enamel thickness on occlusal surfaces with acid challenge involvement are recommended as well as clinical studies for application of PS-OCT to monitor tooth wear.

CONCLUSION

Our findings suggest the potential of PS-OCT as a noninvasive, nondestructive, and reliable method for measuring enamel thickness and for monitoring tooth wear progression on the occlusal surface.

REFERENCES

1. Attin T, Koidl U, Buchalla W, et al. Correlation of microhardness and wear in differently eroded bovine dental enamel. *Arch Oral Biol* 1997;42(3):243-50.
2. Vieira A, Overweg E, Ruben JL, Huysmans MC. Toothbrush abrasion, simulated tongue friction and attrition of eroded bovine enamel in vitro. *J Dent* 2006;34(5):336-42.
3. Ganss C. Is erosive tooth wear an oral disease? *Monogr Oral Sci* 2014;25:16-21.
4. McGuire J, Szabo A, Jackson S, Bradley TG, Okunseri C. Erosive tooth wear among children in the United States: relationship to race/ethnicity and obesity. *Int J Paediatr Dent* 2009;19(2):91-8.
5. Okunseri C, Wong MC, Yau DT, McGrath C, Szabo A. The relationship between consumption of beverages and tooth wear among adults in the United States. *J Public Health Dent* 2015;75(4):274-81.
6. Eccles JTTJopd. Dental erosion of nonindustrial origin. A clinical survey and classification. *J Prosthet Dent* 1979;42(6):649-53.
7. Smith BG, Knight JK. An index for measuring the wear of teeth. *Br Dent J* 1984;156(12):435-8.
8. Lopez-Frias FJ, Castellanos-Cosano L, Martin-Gonzalez J, Llamas-Carreras JM, Segura-Egea JJ. Clinical measurement of tooth wear: Tooth wear indices. *J Clin Exp Dent* 2012;4(1):e48-53.
9. Bartlett D, Ganss C, Lussi A. Basic Erosive Wear Examination (BEWE): a new scoring system for scientific and clinical needs. *Clin Oral Investig* 2008;12 Suppl 1:S65-8.
10. Mulic A, Tveit AB, Wang NJ, et al. Reliability of two clinical scoring systems for dental erosive wear. *Caries Res* 2010;44(3):294-9.
11. Dixon B, Sharif MO, Ahmed F, et al. Evaluation of the basic erosive wear examination (BEWE) for use in general dental practice. *Br Dent J* 2012;213(3):E4.
12. Alves Mdo S, da Silva FA, Araujo SG, et al. Tooth wear in patients submitted to bariatric surgery. *Braz Dent J* 2012;23(2):160-6.

13. Mantonanaki M, Koletsi-Kounari H, Mamai-Homata E, Papaioannou W. Dental erosion prevalence and associated risk indicators among preschool children in Athens, Greece. *Clin Oral Investig* 2013;17(2):585-93.
14. Attin T. Methods for assessment of dental erosion. *Monogr Oral Sci* 2006;20:152-72.
15. Joshi M, Joshi N, Kathariya R, Angadi P, Raikar S. Techniques to evaluate dental erosion: a systematic review of literature. *J Clin Diagn Res* 2016;10(10):ZE01-ZE07.
16. Wilder-Smith CH, Wilder-Smith P, Kawakami-Wong H, et al. Quantification of dental erosions in patients with GERD using optical coherence tomography before and after double-blind, randomized treatment with esomeprazole or placebo. *Am J Gastroenterol* 2009;104(11):2788-95.
17. Chew HP, Zakian CM, Pretty IA, Ellwood RP. Measuring initial enamel erosion with quantitative light-induced fluorescence and optical coherence tomography: an in vitro validation study. *Caries Res* 2014;48(3):254-62.
18. Algarni A, Kang H, Fried D, Eckert GJ, Hara AT. Enamel thickness determination by optical coherence tomography: in vitro validation. *Caries Res* 2016;50(4):400-6.
19. Linkosalo E, Markkanen H. Dental erosions in relation to lactovegetarian diet. *Scand J Dent Res* 1985;93(5):436-41.
20. Lussi A. Dental erosion clinical diagnosis and case history taking. *Eur J Oral Sci* 1996;104(2 (Pt 2)):191-8.
21. Angmar-Mansson B, ten Bosch JJ. Quantitative light-induced fluorescence (QLF): a method for assessment of incipient caries lesions. *Dentomaxillofac Radiol* 2001;30(6):298-307.
22. Pretty IA, Edgar WM, Higham SM. The validation of quantitative light-induced fluorescence to quantify acid erosion of human enamel. *Arch Oral Biol* 2004;49(4):285-94.
23. Lussi A. *Dental erosion: from diagnosis to therapy*: Karger Medical and Scientific Publishers; 2006.
24. Huysmans MC, Thijssen JM. Ultrasonic measurement of enamel thickness: a tool for monitoring dental erosion? *J Dent* 2000;28(3):187-91.
25. Louwse C, Kjaeldgaard M, Huysmans MC. The reproducibility of ultrasonic enamel thickness measurements: an in vitro study. *J Dent* 2004;32(1):83-9.

26. Park J, Choi D-S, Jang I, et al. A novel method for volumetric assessment of tooth wear using three-dimensional reverse-engineering technology: A preliminary report. *Angle Orthod* 2013;84(4):687-92.
27. du Plessis A, Broeckhoven CJAb. Looking deep into nature: A review of micro-computed tomography in biomimicry. *Acta Biomater* 2018.
28. du Plessis A, Broeckhoven C, Guelpa A, le Roux SG. Laboratory x-ray micro-computed tomography: a user guideline for biological samples. *Gigascience* 2017;6(6):1-11.
29. Olejniczaka AJ, Grineb FE. High-resolution measurement of Neandertal tooth enamel thickness by micro-focal computed tomography. *S Afr J Sci* 2005;2:5.
30. Olejniczak AJ, Grine FE. Assessment of the accuracy of dental enamel thickness measurements using microfocal X-ray computed tomography. *Anat Rec A Discov Mol Cell Evol Biol* 2006;288(3):263-75.
31. Kim I, Paik KS, Lee S. Quantitative evaluation of the accuracy of micro-computed tomography in tooth measurement. *Clin Anat* 2007;20(1):27-34.
32. Oi T, Saka H, Ide Y. Three-dimensional observation of pulp cavities in the maxillary first premolar tooth using micro-CT. *Int Endod J* 2004;37(1):46-51.
33. Jafarzadeh H, Wu Y-N. The C-shaped root canal configuration: a review. *J Endod* 2007;33(5):517-23.
34. Balto K, White R, Mueller R, Stashenko P, A mouse model of inflammatory root resorption induced by pulpal infection. *Oral Med Oral Pathol Oral Radiol Endod* 2002;93(4):461-68.
35. de Oliveira KMH, Silva RA, Küchler EC, et al. Correlation between histomorphometric and micro-computed tomography analysis of periapical lesions in mice model. *Ultrastruct Pathol* 2015;39(3):187-91.
36. Huang D, Swanson EA, Lin CP, et al. Optical coherence tomography. *Science* 1991;254(5035):1178-81.
37. Fercher AFJAJO. In vivo optical coherence tomography. *Am J Ophthalmol* 1993;116:113-14.
38. Colston B, Sathyam U, Dasilva L, et al. Dental OCT. *Opt Express* 1998;3(6):230-8.
39. Otis LL, Everett MJ, Sathyam US, Colston Jr . Optical coherence tomography: a new imaging: technology for dentistry. *J Am Dent Assoc* 2000;131(4):511-14.

40. Machoy M, Seeliger J, Szyszka-Sommerfeld L, et al. The use of optical coherence tomography in dental diagnostics: a state-of-the-art review. *J Health Eng* 2017;2017:7560645.
41. Fried D, Xie J, Shafi S, et al. Imaging caries lesions and lesion progression with polarization sensitive optical coherence tomography. *J Biomed Opt* 2002;7(4):618-27.
42. Jones RS, Staninec M, Fried D. Imaging artificial caries under composite sealants and restorations. *J Biomed Opt* 2004;9(6):1297-304.
43. Jones RS, Darling CL, Featherstone JD, Fried D. Remineralization of in vitro dental caries assessed with polarization-sensitive optical coherence tomography. *J Biomed Opt* 2006;11(1):014016.
44. Lee C, Darling CL, Fried D. Polarization-sensitive optical coherence tomographic imaging of artificial demineralization on exposed surfaces of tooth roots. *Dent Mater* 2009;25(6):721-8.
45. Shemesh H, van Soest G, Wu MK, Wesselink PR. Diagnosis of vertical root fractures with optical coherence tomography. *J Endod* 2008;34(6):739-42.
46. Yoshioka T, Sakaue H, Ishimura H, et al. Detection of root surface fractures with swept-source optical coherence tomography (SS-OCT). *Photomed Laser Surg* 2013;31(1):23-7.
47. Na J, Lee BH, Baek JH, Choi ES. Optical approach for monitoring the periodontal ligament changes induced by orthodontic forces around maxillary anterior teeth of white rats. *Med Biol Eng Comput* 2008;46(6):597-603.
48. Baek JH, Na J, Lee BH, Choi E, Son WS. Optical approach to the periodontal ligament under orthodontic tooth movement: a preliminary study with optical coherence tomography. *Am J Orthod Dentofacial Orthop* 2009;135(2):252-9.
49. Ishibashi K, Ozawa N, Tagami J, Sumi Y. Swept-source optical coherence tomography as a new tool to evaluate defects of resin-based composite restorations. *J Dent* 2011;39(8):543-8.
50. Senawongse P, Pongprueksa P, Harnirattisai C, et al. Non-destructive assessment of cavity wall adaptation of class V composite restoration using swept-source optical coherence tomography. *Dent Mater J* 2011;30(4):517-22.
51. de Melo Monteiro GQ, Montes MA, Rolim TV, et al. Alternative methods for determining shrinkage in restorative resin composites. *Dent Mater* 2011;27(8):e176-85.

52. Nakajima Y, Shimada Y, Miyashin M, et al. Noninvasive cross-sectional imaging of incomplete crown fractures (cracks) using swept-source optical coherence tomography. *Int Endod J* 2012;45(10):933-41.
53. Majkut P, Sadr A, Shimada Y, Sumi Y, Tagami J. Validation of Optical Coherence Tomography against Micro-computed Tomography for Evaluation of Remaining Coronal Dentin Thickness. *J Endod* 2015;41(8):1349-52.
54. Se-Ryong K, Jun-Min K, Sul-Hee K, et al. Tooth cracks detection and gingival sulcus depth measurement using optical coherence tomography. *Conf Proc IEEE Eng Med Biol Soc* 2017;2017:4403-06.
55. Imai K, Shimada Y, Sadr A, Sumi Y, Tagami J. Noninvasive cross-sectional visualization of enamel cracks by optical coherence tomography in vitro. *J Endod* 2012;38(9):1269-74.
56. Olejniczak AJ, Grine FE. Assessment of the accuracy of dental enamel thickness measurements using microfocal X-ray computed tomography. *Anat Rec A Discov Mol Cell Evol Biol* 2006;288(3):263-75.
57. Kim I, Paik KS, Lee SP. Quantitative evaluation of the accuracy of micro-computed tomography in tooth measurement. *Clin Anat* 2007;20(1):27-34.
58. Meng Z, Yao XS, Yao H, et al. Measurement of the refractive index of human teeth by optical coherence tomography. *J Biomed Opt* 2009;14(3):034010.
59. Chan KH, Chan AC, Darling CL, Fried D. Methods for Monitoring Erosion Using Optical Coherence Tomography. *Proc SPIE Int Soc Opt Eng* 2013;8566:856606.
60. Bozkurt FO, Tagtekin DA, Hayran O, Stookey GK, Yanikoglu FC. Accuracy of ultrasound measurement of progressive change in occlusal enamel thickness. *Oral Surg Oral Med Oral Pathol Oral Radiol Endod* 2005;99(1):101-5.
61. Lee HS, Kim BI. Assessment of tooth wear based on autofluorescence properties measured using the QLF technology in vitro. *Photodiagnosis Photodyn Ther* 2019.

ABSTRACT

IN-VITRO SIMULATED OCCLUSAL TOOTH WEAR MONITORING BY
POLARIZATION SENSITIVE-OPTICAL
COHERENCE TOMOGRAPHY

by

Ghadeer Alwadai

Indiana University School of Dentistry
Indianapolis, Indiana

Background: Erosive tooth wear (ETW) is the loss of tooth substance due to chemo-mechanical action unrelated to bacteria. ETW affects approximately 46 percent of children/adolescents and 80 percent of adults in the U.S. Visual examination indices are available for the clinical assessment of ETW. Although useful, they are subjective and heavily based on the clinical experience of the examiner. Some quantitative techniques have been proposed and used for clinically assessing erosive tooth wear, including

quantitative light-induced fluorescence, ultrasonic measurement, and more recently, polarization-sensitive optical coherence tomography (PS-OCT).

Objective: The objective of this study was to explore the ability of PS-OCT to objectively measure erosive tooth wear on occlusal surfaces.

Method: This study was conducted in two phases. In the first phase, 10 sound extracted human lower first premolars were selected and then exposed to tooth wear simulation gradually. PS-OCT and micro computed tomography (μ -CT) were used to evaluate enamel thickness of those premolars at the buccal cusp tip during the simulation. In phase 2, 40 extracted human lower first premolars with different severity levels of ETW on occlusal surfaces were selected based on the Basic Erosive Wear Examination (BEWE) index. A total of 10 teeth ($n = 10$) were selected for each BEWE score (0/1/2/3). PS-OCT and μ -CT were used to evaluate the enamel thickness at the highest point on the occlusal surface.

Results: There was good agreement between PS-OCT and μ -CT in both phases (phase 1: 0.89 and phase 2: 0.97) with no significant difference between PS-OCT and μ -CT.

Conclusion: This result shows the potential of PS-OCT as reliable method for measuring enamel thickness and monitoring tooth wear progression on the occlusal surface.

CURRICULUM VITAE

Ghadeer Alwadai

- 1990 Born, Dhahran Aljanoub, Saudi Arabia
- 2008 Completed High School, Dar Al-Erq school, Dhahran Aljanoub, Saudi Arabia
- 2013 BDS, Bachelor of Dental Medicine and Surgery, King Saud University, Riyadh, Saudi Arabia
- 2013 Internship, Aseer Central Hospital, Abha, Saudi Arabia
- 2013 Internship, King Fahad Medical City, Riyadh, Saudi Arabia
- 2014 Teaching assistant, King Khalid University, Abha, Saudi Arabia
- 2019 MSD, Cariology, Operative Dentistry and Dental Public Health Program, Indiana University School of Dentistry, Indianapolis, Indiana

Professional Organizations

American Academy of Operative Dentistry
Saudi Dental Society